MODELLING R-CURVE EFFECTS IN DELAMINATION DAMAGE MECHANISMS

V. Q. Bui [1], E. Marechal [2], H. Nguyen-Dang [3]

[1,3] *Department of Fracture Mechanics-Laboratory of Aeronautic & Spatial Techniques (LTAS)*
University of Liège, 21 Ernest Solvay Street, B-4000 Liège, Belgium
[2] *SAMTECH Company*
25 Frère-Orban Boulevard, 4000 Liège, Belgium

SUMMARY: The presence of imperfect interlaminar interfaces in laminated composites is an essential condition for delamination initiation and propagation. Besides, for a complete characterisation of delamination resistance, the R-curve effect, i.e. the increase of the interlaminar fracture energy G_c as delamination propagates, should be taken into account. Rather than defining the interlaminar fracture energy by one single value G_c, it turns out that both an initiation value G_c (ini), and a steady-state propagation value G_c (s/s-prop) need to be considered. By reducing the description of all interlaminar damage mechanisms within a so-called "equivalent damaged area", damage models associated to weakened interfaces are developed using "steady-state R curves" to simulate the evolution of energy release rates in the damage zone. These models have been integrated into the SAMCEF F.E. package and successfully applied to the modelling of standard delamination tests like Double Cantilever Beam (DCB) and End Loaded Split (ELS) specimens. The importance of taking R-curve effect into account in the numerical simulation is demonstrated by comparing the predicted results with the experimental data.

KEYWORDS: laminates, delamination, damage mechanics, imperfect interface, interface finite element, R-curve, modelling

1. INTRODUCTION

Interlaminar fracture energy G_c is experimentally observed to increase during a delamination process [1,2]. This phenomenon is interpreted as a crack-growth resistance behaviour and is frequently represented by a crack resistance curve referred to as "R-curve", showing that the initial G_c (ini) value at delamination onset, rises up to a steady-state propagation value G_c (s/s-prop).

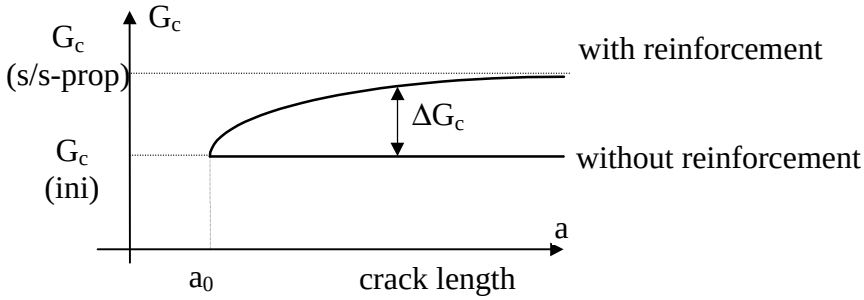

Fig. 1: Evolution of energy release rate during crack growth

Clearly , delamination cannot take place at interfaces where perfect bonding is assumed i.e.; transferring continuous stresses and displacements between adjacent layers. Consequently, the analysis of interlaminar damage mechanisms is most often based on the "imperfect interfaces" concept according to which displacement components υ_i may be discontinuous between adjacent layers, whereas interlaminar tractions t_i remain continuous from simple equilibrium consideration.

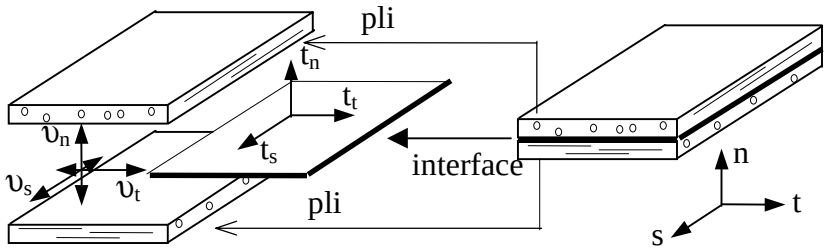

Fig. 2: Displacement jumps and interlaminar tractions at interlaminar interface

Actually, the level of displacement discontinuity between adjacent layers can be simply interpreted as a measure of the interface residual stiffness :

$$d_i = \frac{t_i}{\upsilon_i} \quad (i = n,s,t) \tag{1}$$

The particular case of a perfect interface corresponds to an infinite stiffness $d_i \rightarrow \infty$, and nil displacements discontinuities. Imperfect interfaces are characterized by finite d_i values, hence allowing to model discontinuous displacements $\upsilon_i \neq 0$.

From the above phenomenological observations, the aim of the present work is to develop delamination models based on weakened interface concept and taking R-curve effects into account. They are applied hereafter to the F.E. modelling of standard DCB and ELS delamination test specimens (fig. 3.), respectively dedicated to the assessment of Mode I and Mode II fracture toughness.

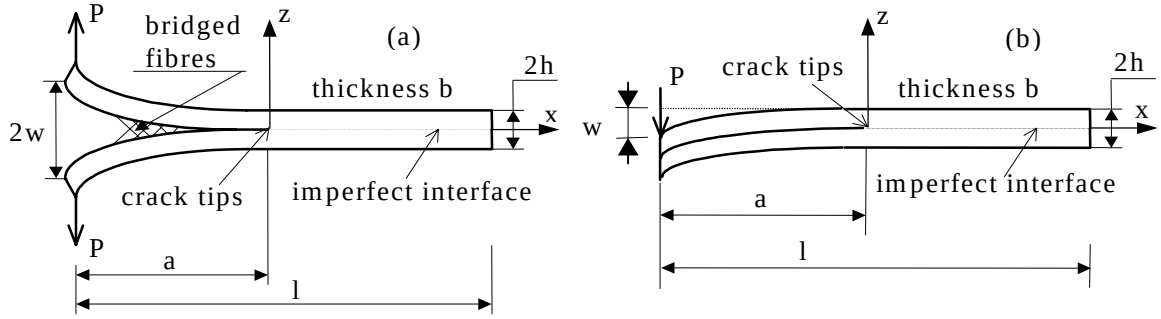

Fig. 3: Configuration of standard delamination specimens
(a) DCB for mode I (b) ELS for mode II

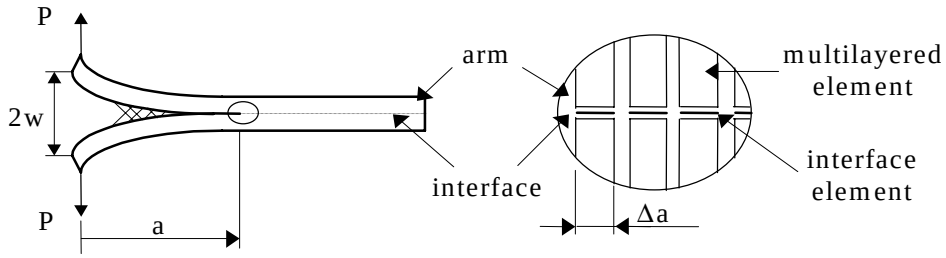

Fig. 4: Finite element discretisation of DCB specimen

The two arms of the beam are modelled using standard 2D multilayered elements, whereas the interface is represented by dedicated zero-thickness elements [4], newly implemented in the SAMCEF F.E. package [3], and to which the below described material models can be assigned [5].

2. MODELS DESCRIPTION

Experimental observations have shown that different forms of damages are present in the vicinity of the crack tip. The adopted methodology consists to gather all micro-cracks and local fractures into an “equivalent” plane damaged area.

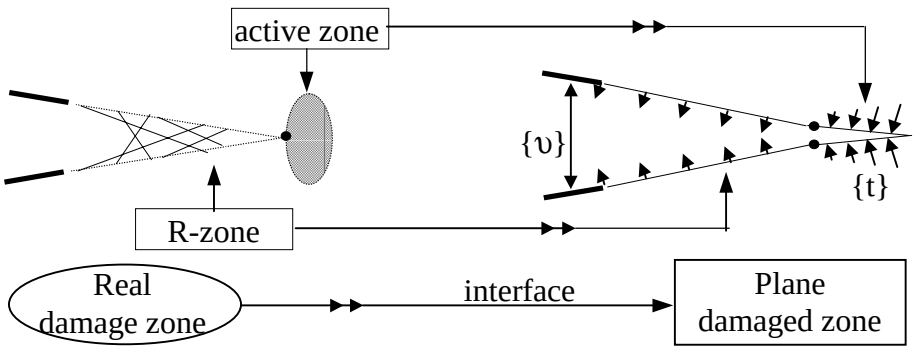

Fig. 5: Damage zone modelling

Damage growth results in reducing interlaminar bonding forces t_i and consequently increasing displacement jumps υ_i. In the absence of reinforcement mechanisms, G_c remains unchanged i.e; $G_c \equiv Gc$ (ini) during the delamination process (fig. 1). In this particular case, the damage zone is approximately constant in size as the crack grows, and is referred to as “active zone” (fig. 5). It is generally accepted that delamination onset occurs if interlaminar stress t_i attains a

critical threshold t_{il} (interfacial strength), and delamination can only propagate if the available energy at interfaces is equal to G_{ic} (ini). If both stress and energy criteria are simultaneously satisfied, we obtain the following debonding model where the stiffness d_i drops instantaneously to zero (fig. 6).

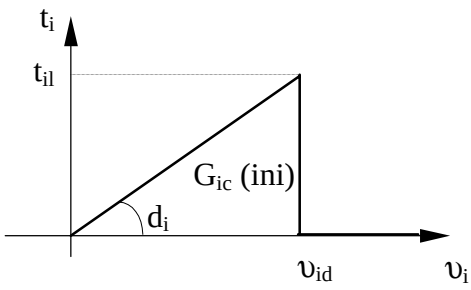

Fig. 6: Debonding behaviour of active zones

Actually, the delamination process is most often monitored by additional energy dissipation sources $\Delta G_c = G_c$ (s/s-prop) – G_c (ini), referred to as "R-curve effects" and confined within so-called "reinforcement zones" (R-zones), in the neighbourhood of the permanent active zone (fig. 5).

Among major R-curve effects, one can distinguish the two following :

- fibre bridges; for general stacking sequences, one often observes unbroken fibres peeled off from the matrix and crossing over the delaminated area (fig. 7). They bridge the two crack lips, which contributes to slow down the propagation process. The corresponding progressive damage model, adopted to simulate this mechanism is illustrated at figure (9.a), showing crack closing forces t_i decreasing linearly according to a given slope s_{ir} .

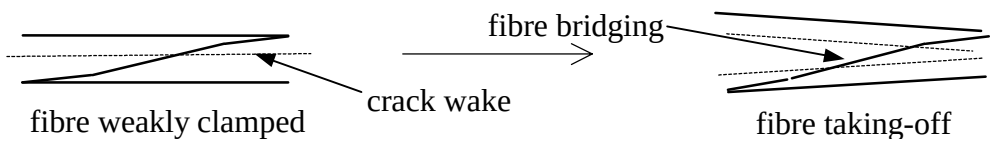

Fig. 7: Fibre bridges

- R-curve effects may also result from a possible excessive plastic deformation of the matrix near the crack tip, leading to the formation of voids and consuming a part of the dissipated energy. When the porosity related to the close neighbourhood of these voids, reaches a certain critical value, all voids coalesce instantaneously , leading to a sudden crack propagation increment (fig. 8).

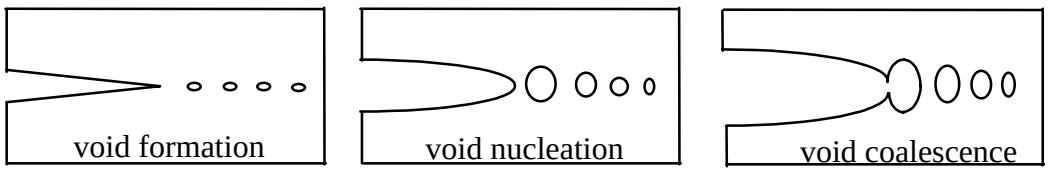

Fig. 8: Voids coalescence process

A so called “brutal” damage model has been developed for this specific type of reinforcement effect; it is illustrated at figure (9.b).

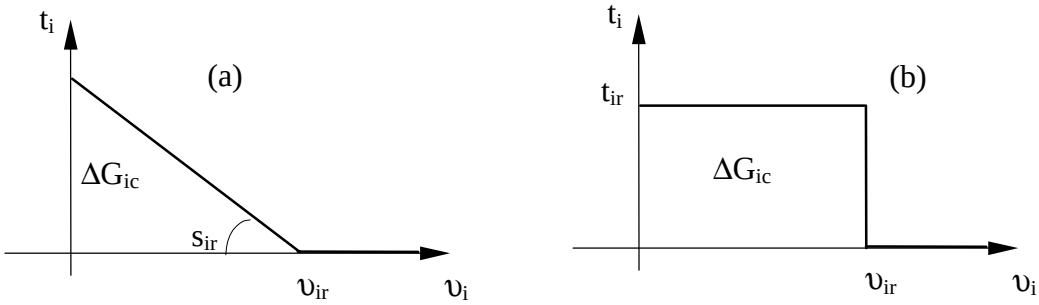

Fig. 9: Reinforcement mechanisms

(a) progressive damage (b) brutal damage

Actually, two models combining the permanent active zone and either of the two reinforcement effects (fig. 10) have been developed and implemented in SAMCEF.

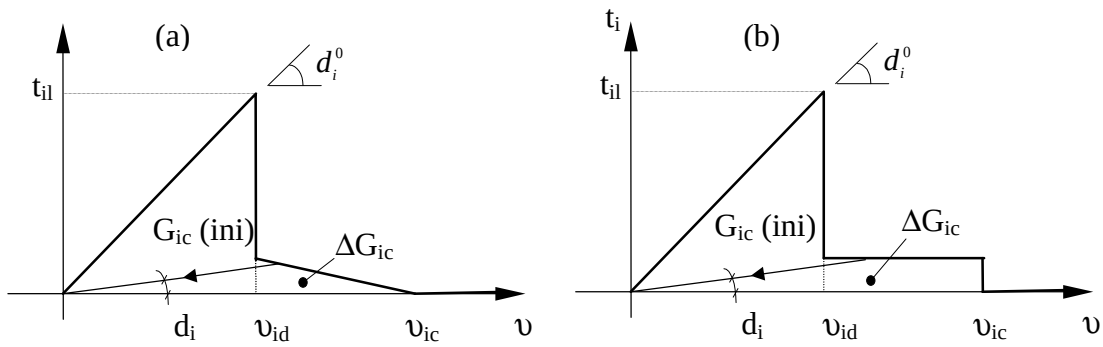

Fig. 10: Damage models combining both active and R-zone effects

The evolution of the interface stiffness d_i during the delamination mechanism can be represented by a very simple law of the following form :

$$d_i = d_i^0 (1 - D_i) \tag{2}$$

where $d_i^0 = \dfrac{t_{il}^2}{2G_{ic}(ini)}$ is the initial stiffness and D_i is a damage indicator, defined as follows for the two respective reinforcement mechanisms :

(i) Debonding model with progressive reinforcement (fig. 10a)

$$D_i = \begin{cases} 0 & , 0 \le \upsilon_i \le \upsilon_{il} \\ 1 - (\dfrac{\upsilon_{ic}}{\upsilon_i} - 1)\dfrac{s_{ir}}{d_i^0} & , \upsilon_{id} \le \upsilon_i \le \upsilon_{ic} \\ 1 & , \upsilon_i > \upsilon_{ic} \end{cases} \tag{3}$$

where

$$\upsilon_{ic} = \sqrt{\frac{2G_{ic}(ini)}{d_i^0}} + \sqrt{-\frac{2\Delta G_{ic}}{s_{ir}}} \tag{4}$$

(ii) Debonding model with brutal reinforcement (fig. 10b)

$$D_i = \begin{cases} 0 & , 0 \le \upsilon_i \le \upsilon_{il} \\ 1 - \frac{t_{ir}}{d_i^0}\frac{1}{\upsilon_i} & , \upsilon_{id} \le \upsilon_i \le \upsilon_{ic} \\ 1 & , \upsilon_i > \upsilon_{ic} \end{cases} \tag{5}$$

where

$$\upsilon_{ic} = \sqrt{\frac{2G_{ic}(ini)}{d_i^0}} + \frac{\Delta G_{ic}}{t_{ir}} \tag{6}$$

3. NUMERICAL RESULTS AND DISCUSSION

Both above described delamination models have been integrated into SAMCEF and assigned to the newly implemented interface elements. They are validated below through numerical simulations of DCB (mode I) and ELS (mode II) standard delamination tests. In order to highlight the contribution of the reinforcement mechanisms to delamination toughness, two analyses (i.e; with and without R-curve effects) were carried out for both tests.

Let us first consider the DCB specimen made from carbon-epoxy (fig. 3a) , used by Robinson and al., [1] to investigate crack jumping and fibre bridging processes in multidirectional laminates. They recorded an R-curve characterised by an initial energy release rate value G_{Ic} (ini) = 0.35 N/mm at delamination onset and G_{Ic} (s/s-prop) = 0.55 N/mm at delamination steady-state growth. The simulation was carried out using the debonding model with progressive reinforcement where a 0.00766 N/mm^3 S_{ir} value was adopted for the slope characterising the linear decreasing of the closing forces versus the crack opening. Besides, we assume t_{nl} = 30 MPa for the interface tensile strength at damage initiation. The size of the smallest elements, next to the crack tip is fixed at Δa = 0.04 mm (fig. 4).

The predicted load versus crack opening path, with and without R-curve effects, is illustrated at figure 11, showing a fairly good agreement with experimental data. As seen at figure 12, the fibre bridging effect clearly slows down the delamination growth. Lastly, figure 13 shows that the evolution of interlaminar fracture energy is also very close to experimental observations.

Similar conclusions can be drawn from the ELS test simulation (fig. 3b), where the reinforcement effect is here mainly due to the excessive plastic deformation of the matrix leading to voids formation in the vicinity of the crack tip. The following respective experimental values were measured for the energy release rates at delamination onset , and steady state crack propagation : G_{IIc} (ini) = 1.23 N/mm; G_{IIc} (s/s-prop) = 1.85 N/mm. The analysis is here performed using the debonding model coupled to a brutal reinforcement effect characterised by a residual shear strength t_{sr} = 7.4 Mpa , the initial shear strength being measured to t_{sl} = 160 Mpa. Similar results as those considered for the DCB specimen are

presented at figures 14 , 15 and 16, showing again the significant contribution of this other type of reinforcement mechanism to the mode II fracture toughness.

The main difficulty in applying the above described models deals of course with the identification of the s_{ir} and t_{ir} parameters related to the progressive and brutal respective reinforcement effects.

The adopted approach to determine these parameters consists in a “trial and error” procedure similar to the one proposed by Demotte and al. [6]. It is briefly described below, in the case of the ELS specimen , for which the t_{sr} brutal reinforcement model parameter needs to be identified (fig 17.) :

(i) From the experimental curve a = a(w), we can extract two displacement values referred to as w_{inf} and w_{sup} between which the first crack growth increment takes place.
(ii) Concurrently, a series of finite element analyses is carried out with different values of t_{sr} and for each of them, the predicted displacement level corresponding to the first crack growth is recorded. From the t_{sr} versus W curve obtained that way, the particular $t_{sr\ inf}$ and $t_{sr\ sup}$ values corresponding to w_{inf} and w_{sup}, can be identified.
(iii) It is then possible to run additional analyses using t_{sr} values ranging from $t_{sr\ inf}$ to $t_{sr\ sup}$, aiming at best fitting the experimental curve and thus determining the final t_{sr} value.

4. CONCLUSIONS

Considering the imperfect interface concept, it was possible to develop damage models taking different types of reinforcement mechanisms into account, which allow to address the full delamination process (i.e; from initiation to propagation) through a new and more realistic approach.

They were successfully applied to the modelling of standard DCB and ELS delamination tests, using dedicated interface elements, newly implemented into the SAMCEF F.E. package.

These two numerical simulations allowed to emphasize the significant contribution of the R-curve effects to the respective modes (i.e; I and II) fracture toughness.

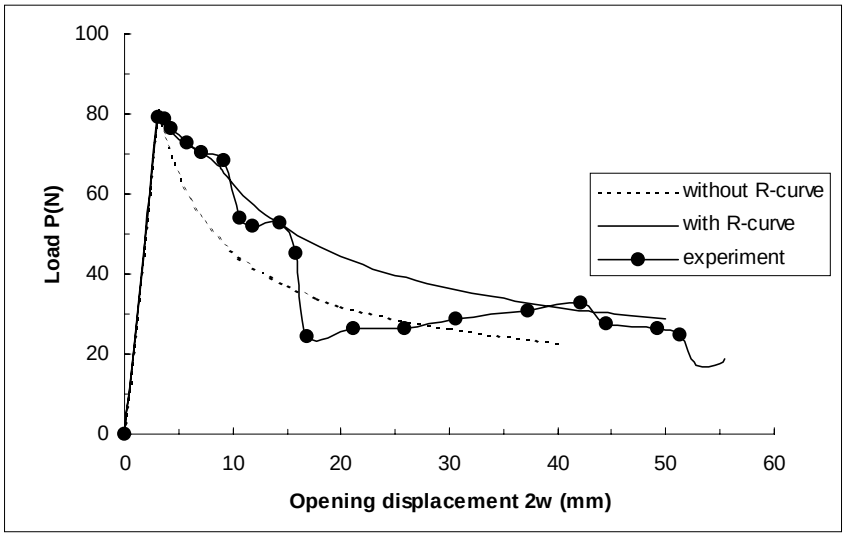

Fig. 11: DCB specimen – Load versus opening displacement.

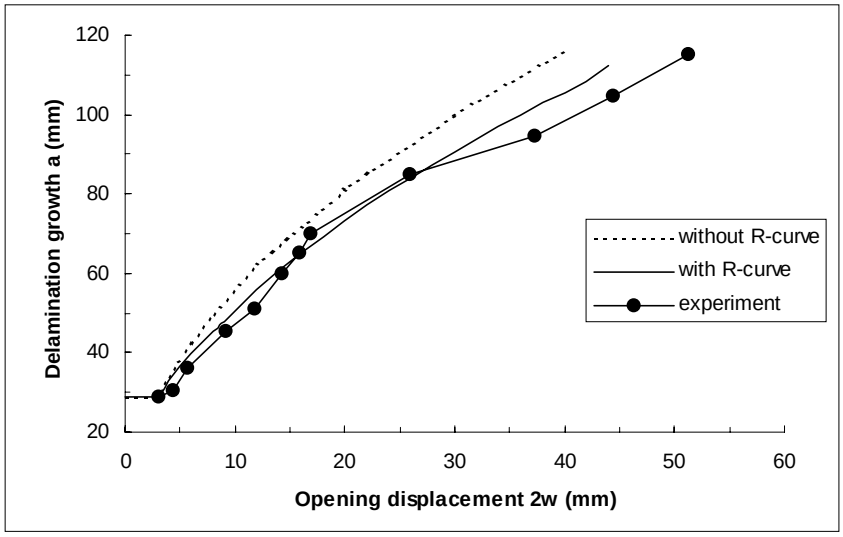

Fig. 12: DCB specimen – Crack growth versus opening displacement.

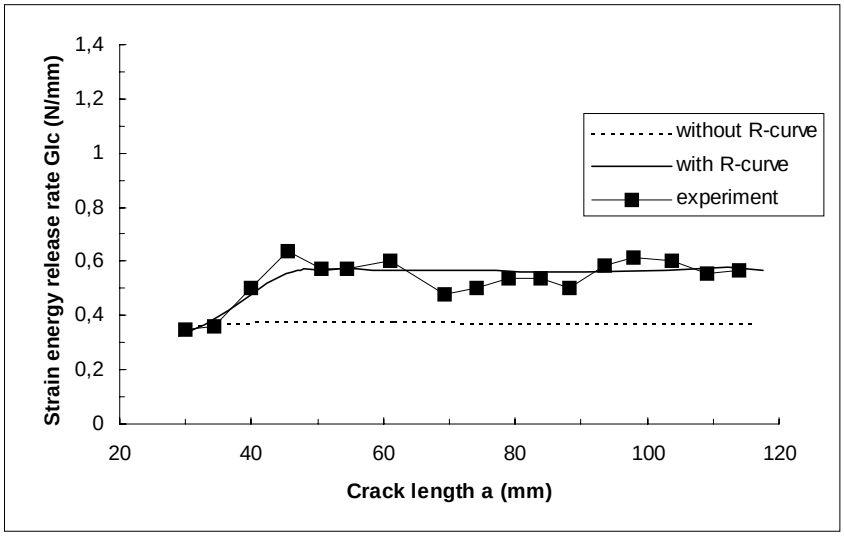

Fig. 13: DCB specimen – Energy release rate versus crack growth.

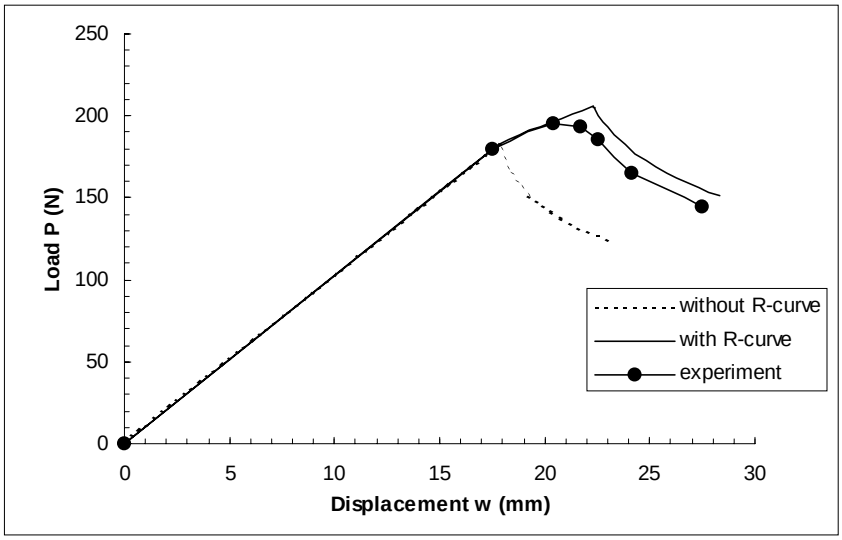

Fig. 14: ELS specimen - Load versus displacement path.

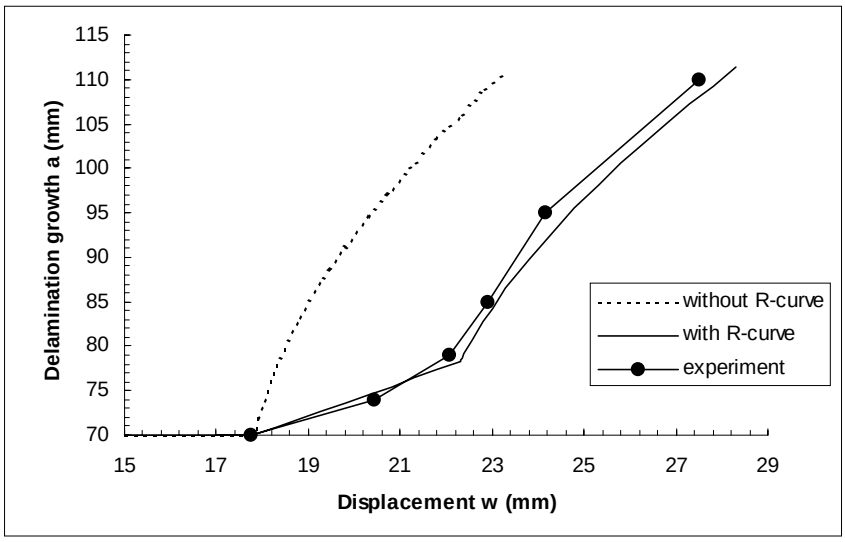

Fig. 15: ELS specimen – Crack growth versus displacement path.

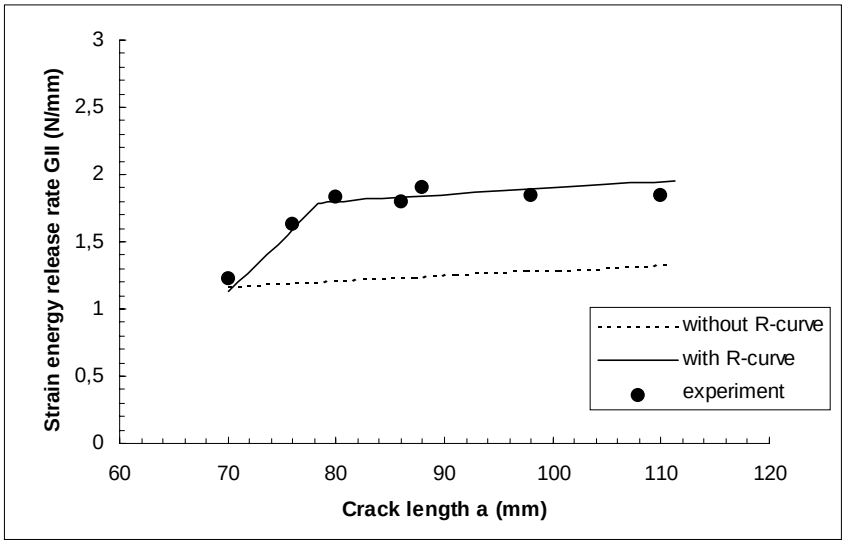

Fig. 16: ELS specimen – Energy release rate versus crack growth.

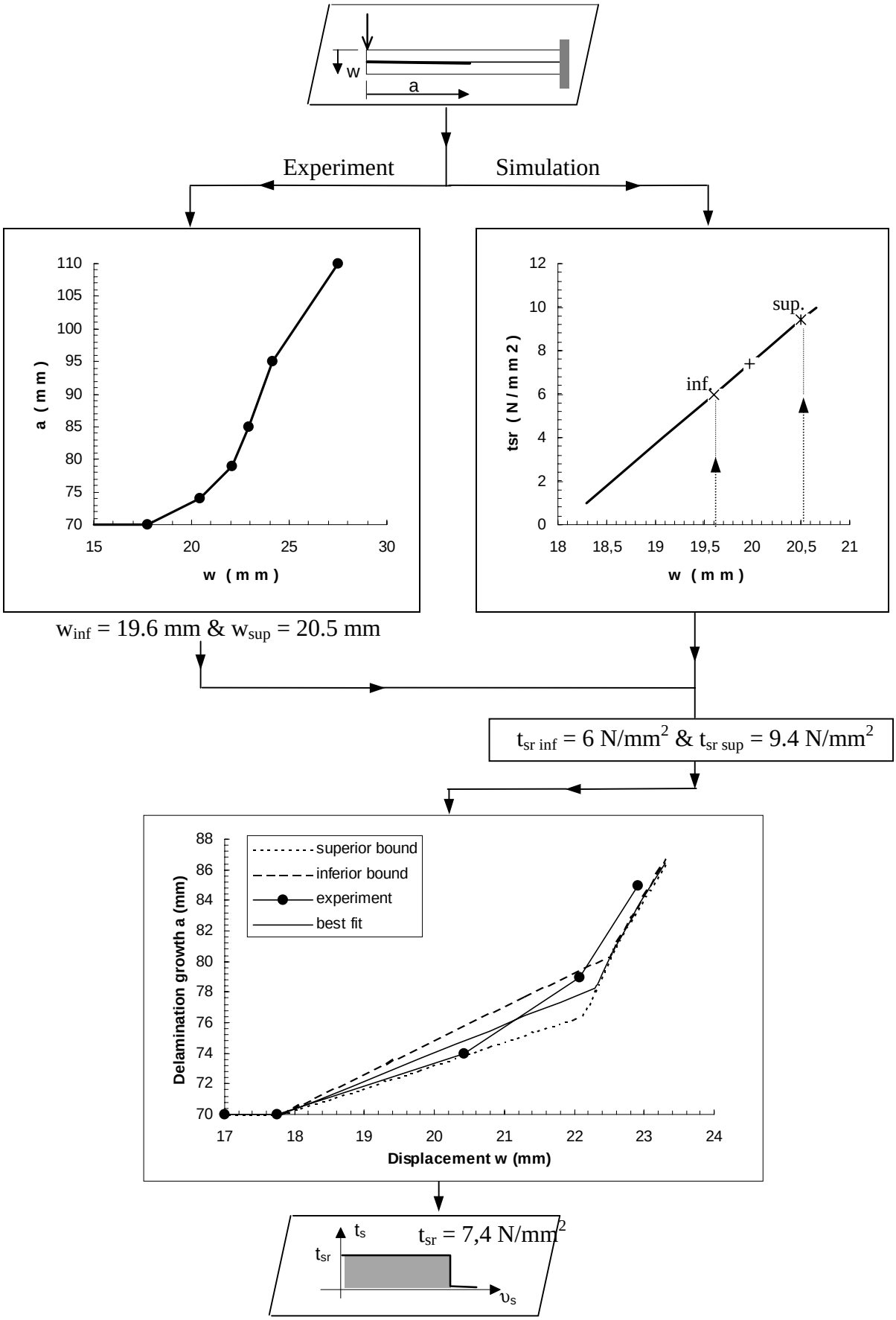

Fig. 17: Determination of the brutal reinforcement model t_{sr} parameter for the ELS specimen

REFERENCES

1. Robinson P. and Song D. Q., "A modified DCB specimen for mode I testing of multidirectional laminates", *Journal of Composite Materials*, Vol. 26, 1992, pp. 1554-1577.

2. Hashemi S., Kinloch A. G. and Williams J. G., "Mechanics and mechanisms of delamination in a poly(ether sulphone)-fibre composite", *Composites Science and Technology*, Vol. 37, 1990, pp. 429-462.

3. Samtech, Composites-SAMCEF Users manual M9, release 7.1, 1997

4. Bui Q. V., Marechal E. and Nguyen-Dang H., "SAMCEF/COMPOSITES: modelling delamination initiation and propagation in layered composites using interface elements", *Samtech Users'Conference Proceedings*, Liège, Belgium, October 21-22, 1998.

5. Bui Q. V., "Modélisation de l'interface imparfaite interlaminaire dans l'étude du délaminage des stratifiés composites", *Ph. D. thesis*, University of Liège, Belgium, December 1998.

6. Demotte J., Roelandt J. M. and Abisror A., "A numerical analysis to assess ductile tearing in thin plates using local approach application to R curve simulation", *Proceeding of the 5th International Conference in Numerical Methods in Fracture Mechanics*, Luxmoore A. R. and Owen D. R. J., Eds, 1990, pp. 631-643